2023 IEEE International Conference on Robotics and Automation (ICRA 2023)
May 29 - June 2, 2023. London, UK

Origami Folding Enhances Modularity and Mechanical Efficiency of Soft Actuators

Zheng Wang
National University of Singapore (Suzhou) Research Institute
Suzhou, China
wangzheng@u.nus.edu

Yazhou Song
National University of Singapore (Suzhou) Research Institute
Suzhou, China
e1010761@u.nus.edu

Zhongkui Wang
Department of Robotics Ritsumeikan University
Kusatsu, Japan
wangzk@fc.ritsumei.ac.jp

Hongying Zhang
Department of Mechanical Engineering National University of Singapore
Singapore
hy.zhang@nus.edu.sg

***Abstract*—Soft robots have long been attractive to robotic engineers due to their remarkable dexterity; however, reports that standardize soft actuators into modularized off-shelf devices akin to rigid robots are still rare, and the mechanical efficiency of existing designs is still limited. This work identifies origami folding to enable the design of LEGO-like modularized soft actuators with high mechanical efficiency in terms of payload capability and workspace. Herein, three modularized origami actuators that can generate translational, bending, and twisting motion are designed, prototyped, and tested. The translational actuator can contract to 40% of its original length, and the twisting and bending actuators can exert 31° and 52° angular motions, respectively. The translational actuator can exert a blocked force of about 821 times self-weight. The motion of origami soft actuators is accurately modeled using rigid body kinematics, and complex systems built by them are captured by homogeneous transformation. Finally, the modularized design and efficient kinematic model are verified on a manipulator and a reconfigurable letter. Benefiting from the unprecedented modularity and mechanical efficiency, these LEGO-like origami actuators are promising for practical applications like food handling and healthcare.**

Keywords*—Soft Actuators, Origami Folding, Modularity, Mechanical Efficiency

I. Introduction

The conventional rigid-bodied robots are built-up with rigid links and joints, which are difficult to be used in unstructured environments that require high adaptability and safe interaction with humans. Soft robotics is emerged as a promising solution to overcome the drawbacks of rigid robots and has been extensively studied in the past two decades [1], [2]. Soft robots are essentially made of flexible and/or soft materials that can deform and absorb much of the energy arising from collisions. The intrinsic softness equips the soft robots with a continuously deformable structure that can mimic the muscular organs of biological systems and gain a relatively large number of degrees of freedom (DOF) compared to their rigid counterparts [2].

The intrinsic coupling of material, structure, and actuation brings unprecedented challenges to the design of soft robots [3]. Robotic designers usually rely on intuitions, experiences, or bio-inspiration to design the structure of soft robots, which can provide only limited scope. For instance, the two most widely used soft actuator designs: PneuNets and fiber-reinforced structures, deform along the low stiffness direction upon actuation to give rise to bending, contraction, or twisting motion [4]-[7]. Their mechanical performance in terms of motion and payload is deeply coupled with the structure and material, making the design of a soft robot with complex motions more challenging as simply superposition is not applied to the existing designs. Additionally, the basic kinematics applicable to rigid robots is invalid for soft robots due to their intrinsic softness, and an efficient model to capture the complex kinematic motions of soft robots is still missing [8]. Apart from the structure design, the low payload capacity remains a critical challenge in practical applications, which is less than 10 N for the majority of existing designs [9]-[11]. Herein, we identify origami folding to overcome the listed challenges in modularized structure design, mechanical efficiency, and kinematics model.

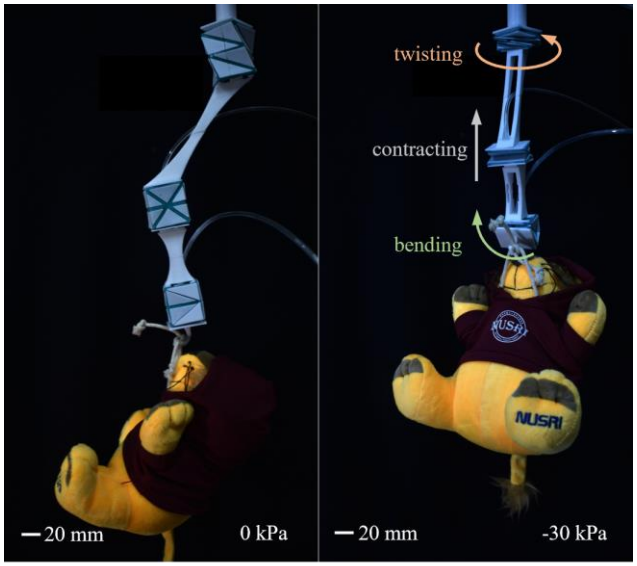

Fig. 1. A robotic manipulator built by modularized origami soft actuators is able to lift a toy. (a) The robotic manipulator at the initial state and (b) actuated state.

The origami folding principle, involving folding ("ori") two-dimensional paper ("kami") into complex three-

dimensional shapes, has been long inspiring engineers to design compact kinematic structures [12], [13]. The basic structure of origami is simply a collection of spatially organized folds, which can be classified into mountain folds and valley folds based on the folded configuration, either convex or concave shape, respectively [12], [14]. The physical origami structures normally consist of rigid panels and compliant fold regions, which are also known as hinges. The compliance of the hinges ensures safe interaction with humans and the environment, while the rigid parts enable high mechanical efficiency and motion accuracy. Utilizing this simple folding principle, many origami-based robots and actuators have been developed to solve aforementioned problems. For instance, origami-based bellows have been proven that can be used to realized different kinematic motions, and they can be activated by multiple methods, e.g., pneumatics [15], [16], cable-driven [17], [18], and magnetics [19]. Although the versatility of origami patterns has been verified in these works, their ability to be used as modularized actuators akin to LEGO-like building blocks is yet to be demonstrated.

Herein, we design three modules of soft actuators using origami folding to generate contraction, bending, and twisting motion, respectively. Providing the facets are made of rigid materials, the physical origami structures will merely fold along the hinges without deformation on the facets during the motion, which means the rigid body kinematics and supervision principle are also valid in modeling the kinematic motion of origami soft actuators. Hence, we use the homogeneous matrix to model the kinematic motion of origami soft actuators in this work. Additionally, we can build complex semi-soft robot systems using the three proposed modules by decomposing the motion into basic contraction, bending, and twisting motions, and model their kinematics using the superposition principle, taking the robotic arm shown in Fig. 1 as an example.

To characterize the mechanical efficiency and verify the modularized design principle, we prototype three origami soft actuators using a lamination technique [20]. Herein, we prepare the rigid origami panels using 3D printing, then tessellate the facets onto TPU-coated fabric using hot-pressing, and finally, fold the tessellation and seal the soft actuator to ensure airtightness using ultrasonic welding. To evaluate the workspace, we conducted 300 times of repeatable free travel tests. The experimental results show that the translational actuator contracts to 40%±0.5% of its original length, while the twisting and bending actuators can exert 31°±0.6° and 52°±0.6° angular motions within 300 times working cycles. Regarding the payload capacity, we tested the blocked force of these actuators in different pre-deformation states. The experiments reveal that the contraction actuator can generate a peak blocked force of 78 N at -50 kPa, which is 821 times of its self-weight (9.5 g). Our work here demonstrates the potential of applying origami structures in the field of soft actuators and soft robots.

The main contributions of this letter are as follows:

- three types of modularized origami soft actuators with high mechanical efficiency;
- a comprehensive model to simulate the kinematics of the modularized soft actuators and complex systems based on them;
- experimental characterization and demonstration of the modularized design principle and kinematic model

II. Structure Design and Kinematics Modeling

A. Design of the Two-dimensional Folding Patterns

The principles of origami folding are leading to paradigm shifts in the design, fabrication, and perception of structures and machines. In theory, by rationally designing the spatial distribution of folds, any complex 3D geometry can be created by folding a thin sheet [12]. The basic technique of origami folding is simple: fold a planar sheet either into or out of the plane to form a convex (mountain) and concave (valley) hinge shape, one being the inverse of the other. However, variation and complexity arise when multiple folds come to interact together [21], [22]. So far, master artisans of origami have passed down tradecraft to select a few kinematic origami patterns for engineering applications to generate different types of motions [22]. However, a generalized principle to convert these patterns into practical soft actuators is still missing.

In conventional rigid robotic systems, complex motions are normally decomposed into a combination of prismatic

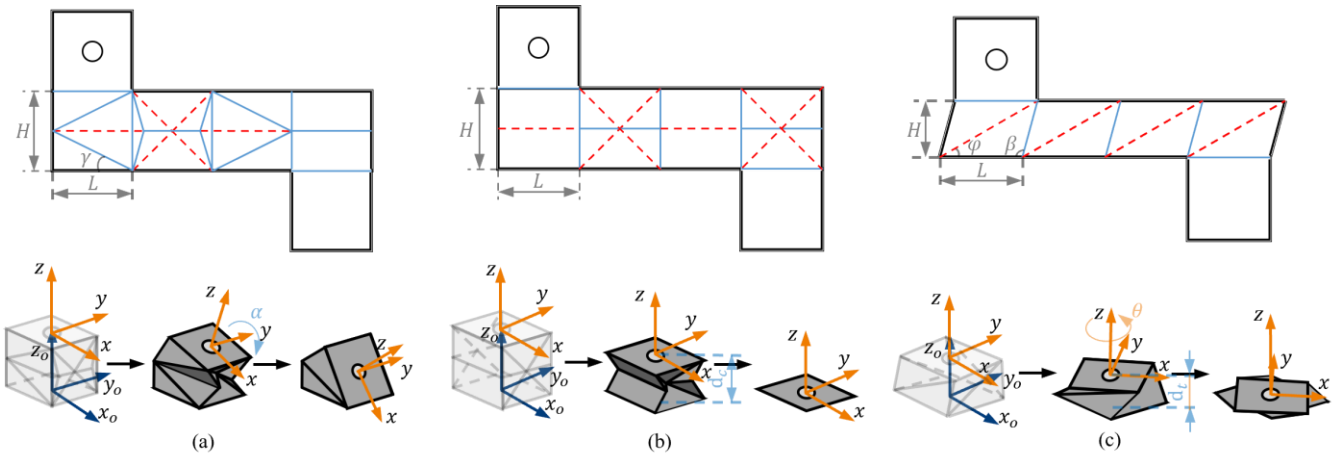

Fig. 2. The 2D folding pattern and folded configurations of the proposed soft actuators, including (a) a bending, (b) contraction, and (c) twisting actuator, respectively. In all the folding patterns, the red dotted lines represent the valley creases and the solid blue lines represent mountain creases, and black solid lines are the glued boundaries.

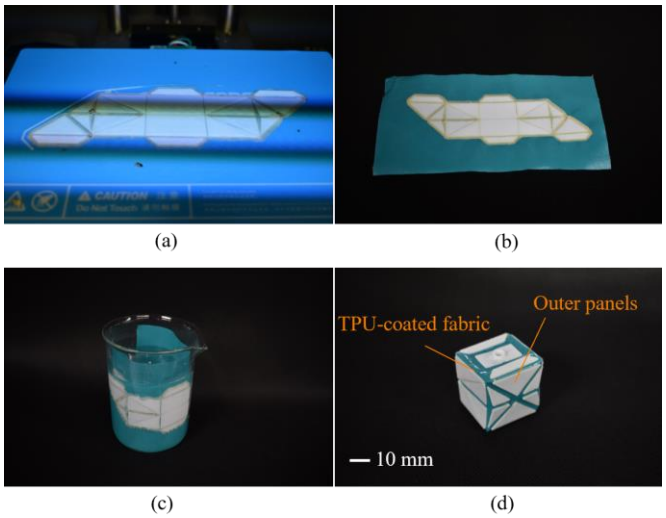

Fig. 3. The fabrication process of the origami actuators. The main steps are: (a) 3D printing the facets with supportive materials for positioning; (b) tessellating the facets onto TPU-coated fabric by thermo-compression; (c) dissolving the supportive materials; (d) and finally fold the pattern and seal the actuator.

and rotational motions. To simplify the structure design of soft robots, we introduce this modularization concept to develop soft actuators. As shown in Fig. 2, we propose two new patterns and a variation of the Kresling pattern [23], [24] to achieve linear contraction, bending, and twisting motion, respectively. Additionally, to ensure the off-shelf assembly of modularized actuators to build complex systems, we require the cross-section of the bases to be identical, i.e., square shape in this work.

As shown in Fig. 2(a), to create a bending motion of the top base with respect to the bottom base, we tessellate the collapsed side face with a waterbomb unit [25], which is composed of four valley folds and two mountain folds that can generate three DOFs of motion, i.e. one symmetric bending and two asymmetric twistings. Hence, it is necessary to introduce a symmetric constraint to the waterbomb unit to ensure pure bending. As shown in Fig. 2(a), it is achieved by adding rational folding designs to the adjacent and opposite side faces. The kinematics of the bending module is determined by the height, H, and length, L. The higher the ratio of height over length, the larger the bending workspace for the origami actuator. To be noted, the hole on the top facet serves as the pressure inlet.

Similar to the bending pattern, the folding pattern of the contraction module is also based on the waterbomb unit [25], as shown in Fig. 2(b). Herein, two opposite side faces are tessellated with waterbomb units, and the remaining two faces are tessellated with parallel folds. The kinematic motion of the contraction actuator is determined by the height, H, and length, L, as illustrated in Fig. 2(b). The actuator undergoes contraction while preserving the diameter of the cross-section, making it superior to the widely used McKibben muscles in mechanical efficiency. Regarding the twisting actuator, we adopt the widely used Kresling pattern, which is built by compressing thin-walled cylinders with distortion on the ends [22], [26]. To ensure the consistency of the cross-section for all three modules, we make a variation to the basic Kresling folding pattern [23], which is shown in Fig. 2(c), as well as its kinematic motion. To be noted, axial contraction is also inevitable when the actuator produces twisting motion. The kinematic twisting motion is characterized by the height, H, length, L, and two section angles between the folds and boundaries, φ and β.

B. Kinematics modeling

The proposed origami actuators are assumed to be rigidly foldable, which means that they can only fold without inducing any facet deformations. Hence, we can use rigid body kinematics to analyze their motions. The kinematic model of the soft origami actuators is crucial as it permits the understanding of how to assemble the modularized actuators to generate complex motions. Without considering the thickness of the origami facets, the width of the folds, and constituent materials, the single DOF origami actuators can be described using the homogeneous transformations, which can be calculated by

$$ {}^{i-1}_{i}T = \begin{bmatrix} {}^{i-1}_{i}R & {}^{i-1}_{i}P \\ 0 & 1 \end{bmatrix} \tag{1} $$

where ${}^{i-1}_{i}T$ is the homogeneous transformation matrix from the $(i-1)$-th coordinate frame to the i-th coordinate frame. ${}^{i-1}_{i}R$ and ${}^{i-1}_{i}P$ are the rotation matrix and the position from the $(i-1)$-th coordinate frame to the i-th coordinate frame, respectively.

The global coordinate systems for each module are specified in Fig. 2, where the origin is attached to the center of the bottom base, and the z-axis is along the height direction, the coordinate system $x_0y_0z_0$ is attached to the bottom base and xyz is attached to the top base. By substituting to (1), the homogeneous transformation matrix of motion on the top base is denoted as

$$ \begin{cases} T_{trans}(d_c) = \begin{bmatrix} 1 & 0 & 0 & 0 \\ 0 & 1 & 0 & 0 \\ 0 & 0 & 1 & d_c \\ 0 & 0 & 0 & 1 \end{bmatrix} \\ T_{bend}(\alpha) = \begin{bmatrix} \cos\alpha & 0 & \sin\alpha & \frac{H}{4}\sin 2\gamma \\ 0 & 1 & 0 & 0 \\ -\sin\alpha & 0 & \cos\alpha & \frac{H}{2}\cos^2\gamma \\ 0 & 0 & 0 & 1 \end{bmatrix} \\ T_{twist}(\theta, d_t) = \begin{bmatrix} \cos\theta & -\sin\theta & 0 & 0 \\ \sin\theta & \cos\theta & 0 & 0 \\ 0 & 0 & 1 & d_t \\ 0 & 0 & 0 & 1 \end{bmatrix} \end{cases} \tag{2} $$

where d_c is the distance between the top and the bottom facet of the contraction actuator, α is the bending angle, θ is the twisting angle, d_t is the axial contraction distance during the twisting motion, and $\tan\gamma = \frac{H}{2L}$, which are all indicated in Fig. 2 The kinematics of a complex system created by assembling the modularized actuators in series can be calculated by simply multiplying the homogeneous transformation matrices accordingly.

III. Fabrication and Characterization Tests

A. Fabrication and Material Choices

To ensure rigid foldability of the origami actuators, their

facets are required to be made of non-deformable materials, then the deformations are restricted to the hinges. Herein, we use 3D printable PLA for the facets and flexible thermoplastic polyurethane-coated nylon fabric (TPU-coated fabric) for the hinges. To ensure airtightness, the TPU-coated fabric forms a closed air chamber and the PLA facets are tessellated onto the TPU-coated fabric by thermo-compression. It is crucial to establish an efficient approach to position the isolated facets onto the TPU-coated fabric to ensure the high fidelity of the fabrication process. Herein, we take advantage of the support material in 3D printing to ensure the accurate position of the panels. Thereafter, the support structure will be removed after the panels are bonded to the fabric. Although some traditional positioning approaches also can be used to accomplish this task, such as bolt positioning [27], some holes will be left on the surfaces, which requires extra work to ensure airtightness and may induce some shape errors. Therefore, the origami actuators can be prototyped with high fidelity and efficiency.

The prototyping process is divided into four basic steps, as shown in Fig. 3. Firstly, fabricating the PLA panels with a thickness of 1mm using a 3D printer (Flashforge Creator Pro 2). Herein, the dissolvable PVA support structures are remained after removing the parts from the printer. Then, tessellating the panels to TPU-coated fabric using a hot-pressing machine at 180 ℃ for 15 seconds. Thirdly, dissolving the support material in water. Finally, folding the tessellation and sealing two bases and side edges using an ultrasonic welding machine. As shown in Fig. 3, the prototyped origami actuators are initialized at the undeformed state, hence negative pressure is applied to the actuators to coordinate the motions.

B. Blocked Force Tests

The modularized origami-based actuators are designed to be of high mechanical efficiency in a way that they can exert a high payload and undergo a large range of motion. With these advantages, these proposed soft actuators are expected to be applied to build lightweight grippers or manipulators and compact reconfigurable robots. To evaluate their performance, we characterize their payload capability and workspace. The experimental setup for the payload capability characterization is shown in Fig. 4, where the motion of the actuator is constrained by two clamps upon actuation of various negative pressure. The pneumatic actuation system consists of an air pump, a proportional valve, and a pressure sensor. The air pump can produce a vacuum pressure of -80kPa at a flow rate of 15 L/min. The proportional valve (SMC ITV2090-212CL5) can control the negative pressure

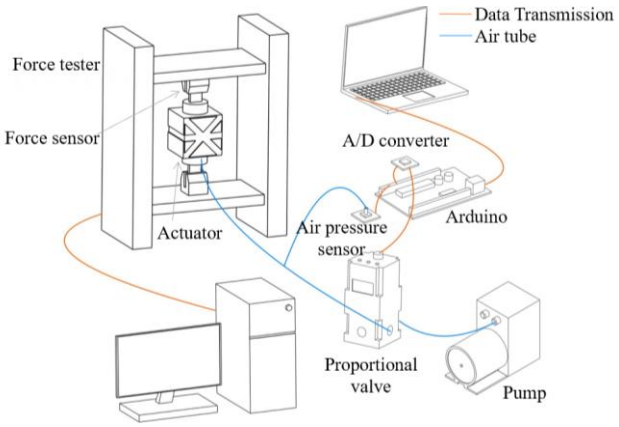

Fig. 4. The experiment setup for the payload capability, where the origami actuators are clamped on an Instron machine, and the blocked force under various actuation pressure are recorded.

change from 0 to -50 kPa at a rate of 1.67 Pa/s. A pressure sensor and a force sensor are used to measure and record the pressure and the blocked force simultaneously.

To evaluate the blocked force, each origami actuator goes through three repeatable tests, and the experimental results are elaborated in Fig. 5. It is observed that the contraction actuator can generate a blocked force as high as 78 N under -50 kPa as indicated in Fig. 5(a), which is 821 times of its self-weight, 9.5 g; and the bending actuator can also exert 46.6 N blocked force at -50 kPa with a payload over weight ratio at 537, as shown in Fig. 5(b). Additionally, we also investigate the load capacity under different pre-deformations. As shown in Fig. 5, the blocked force generated by the actuators decreases as pre-deformation increases because of the reduction of motion range. For instance, under a pre-contraction of 15 mm, the blocked force generated by the contraction actuator reduces to 14 N at -50 kPa; and a 12.4 N blocked force is generated by the bending actuator at a pre-bending of 30°. Nonetheless, the actuators can still generate a blocked force more than 100 times its self-weight.

C. Workspace Characterization

To evaluate the workspace of the proposed origami actuators, we conducted 300 times of repeatable free travel tests for each actuator, and capture the motion range every 25 times. The initial height of the contraction actuator is 40 mm, and it can generate a 24 mm contraction at -20 kPa as shown in Fig. 5(c). Considering the thickness of the panels is 1 mm, the maximal contraction rate achieved is 60%±0.5% as shown in Fig. 6(a), which is far superior to conventional McKibben muscles whose contraction ratio is less than 25% [28]. The physical bending actuator with thick panels can

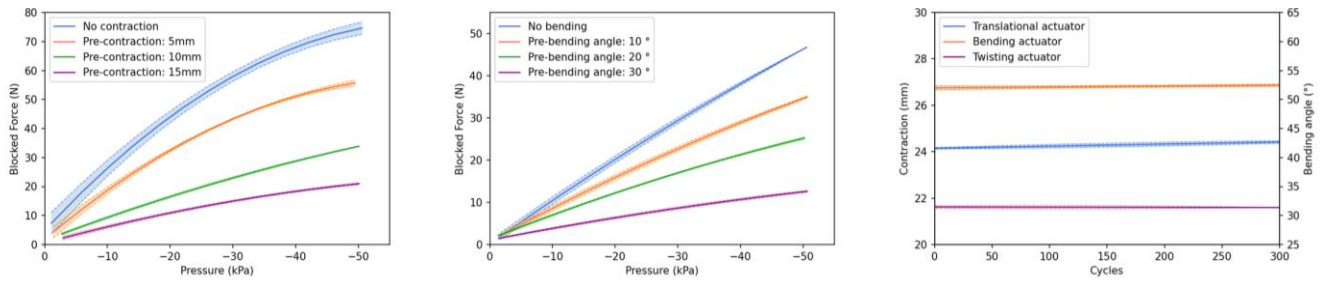

Fig. 5. The characterization tests for three modularized origami actuators, including the blocked force for (a) contraction actuation and (b) bending actuator under different pre-contractions, respectively; and (c) the maximal range of motion of three actuators during 300 times repetitive tests.

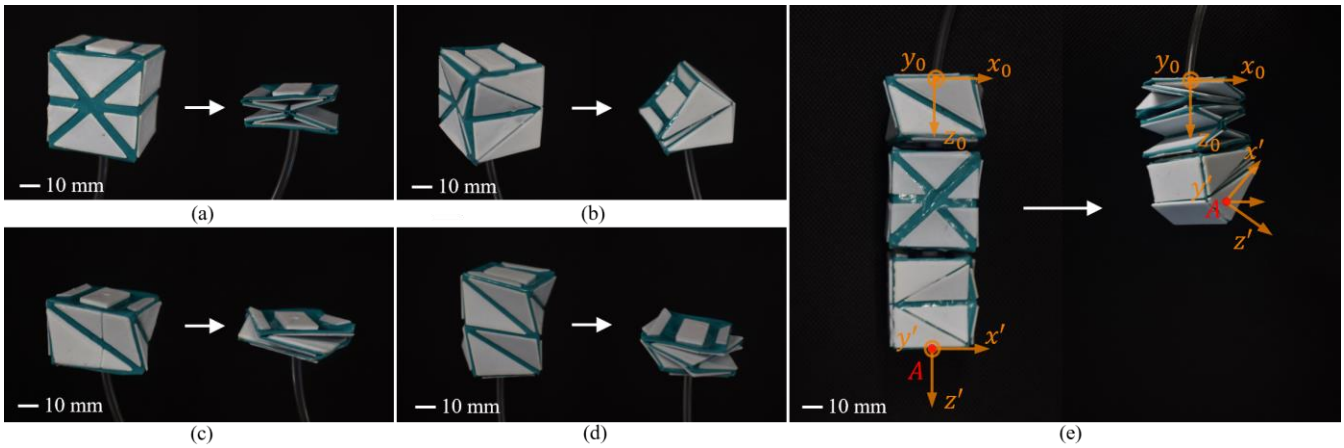

Fig. 6. The configurations of origami actuators in the initial and fully folded state for the (a) contraction actuator, (b) bending actuator, (c) twisting actuator and two assembled system, including (d) double-layer twisting actuator and (e) combination of three origami actuators.

undergo an α=52.1 ° ± 0.7 ° bending under -20 kPa as shown in Fig. 5(b). Regarding the twisting actuator shown in Fig. 6(c), it can generate a θ=31.4° ± 0.7° twisting motion at -20 kPa. To be noted, the maximal motion deviations for all three types of origami actuators are within 2.2%, which indicates extremely high repeatability and motion accuracy.

D. Programmable Motions

Akin to modularized designs in rigid robots, these proposed actuators can also be assembled to build a complex system to fulfill desired motions. For example, two layers can be added to amplify the workspace, as shown in Fig. 6(d); and the three types of soft actuators can also be assembled together to build a three DOF structure, as shown in Fig. 6(e). Rather than re-modeling the new complex system in conventional soft robots, we can directly model its kinematics using the homogeneous transformation. For instance, the position of Point A in the center of the bottom base for the system shown in Fig. 6(e) can be computed by

$$ {}^{0}_{A}P = T_{twist}(\theta, d_t)T_{trans}(d_c)T_{bend}(\alpha){}^{3}_{A}P = \begin{bmatrix} 6.73 \\ -4.11 \\ 40.16 \\ 1 \end{bmatrix} \quad (3) $$

where $T_{twist}(\theta, d_t)$, $T_{trans}(d_c)$, and $T_{bend}(\alpha, \gamma)$ are described in (2), with θ= -31.4°, α=52.1°, H=40 mm, d_t=8 mm, d_c =16 mm, and $\tan\gamma = 0.5$ according to the experimental results; ${}^{3}_{A}P = [0 \quad 0 \quad 0 \quad 1]^T$ is the position of point A in the local coordinate system of the bending actuator, $x'y'z'$, and ${}^{0}_{A}P$ is the position of point A under the global coordinate system, $x_0y_0z_0$.

IV. Applications

The characterization tests reveal that the modularized origami actuators can carry high payloads and generate a large workspace with impressive repeatability and accuracy, which lay the foundations for applying them in practical scenarios. For instance, to design a manipulator for food handling, the engineer merely needs to decompose the complex handling motion into three basic motions, i.e. contraction, bending, and twisting, then assemble the modularized origami actuators at the corresponding positions. Finally, actuate and control the system to fulfill desired tasks. Similar to the programmable motion in Section III, we can also model the kinematic motion of the complex system using the homogeneous transformation based on the model depicted in (2). In this work, we demonstrate the modularized design principle and efficient kinematics modeling of these modularized origami actuators on a robotic arm and reconfigurable robot.

A. Robot Arm

As shown in Fig. 7(a), the robotic arm consists of three modularized origami actuators with three types, i.e. a 2-layer twisting actuator, a translational actuator, and a bending actuator, 3D printed rigid links joining the modularized origami actuators, and a hook at the end to lift target objects. Herein, the modularized actuators are connected to the same pressure source and actuated simultaneously; but individual control is also achievable by redesigning the pneumatic actuation circuit. Upon a vacuum pressure of -30 kPa, a mug (Fig. 7(b)) and a mass weighting 0.5 kg (Fig. 7(c)) are lifted. The kinematic motion of the robot arm can be obtained using homogeneous transformation by multiplying the matrix depicted in (2) for each origami actuator. Herein, the kinematic motion of this robotic arm, denoted by the position of point A, can be computed by

$$ {}^{0}_{A}P = T_{twist}(\theta, d_t)T_{twist}(\theta, d_t){}^{2}_{3}TT_{trans}(d_c){}^{4}_{5}TT_{bend}(\alpha){}^{6}_{A}P = \begin{bmatrix} 40.17 \\ -78.16 \\ 188.16 \\ 1 \end{bmatrix} \quad (4) $$

where $T_{twist}(\theta, d_t)$, $T_{trans}(d_c)$, and $T_{bend}(\alpha, \gamma)$ are calculated by substituting the parameters into (2) with θ= -31°, α=52.1°, H=40 mm, d_t=8 mm, d_c=16 mm, and $\tan\gamma = 0.5$ according to the experimental results. ${}^{2}_{3}T$ and ${}^{4}_{5}T$ are the transformation matrixes of two linkages, respectively, and they can be computed by substituting the parameters illustrated in Fig. 7(a) into (1), with h_1 =80 mm, h_2 =60 mm, and l = 80 mm. ${}^{6}_{A}P = [0 \quad 0 \quad 0 \quad 1]^T$ is the position of point A in the local coordinate system of the bending actuator; and ${}^{0}_{A}P$ is the position of point A in the global coordinate system. Although the structure is simple, this robotic arm demonstrates the potential for applying the proposed soft actuators in food handling or other relevant scenarios. Benefiting from the built-in compliance of hinges, the robotic arm can also ensure safe interaction with the environment.

B. Reconfigurable Letter

To further demonstrate the modularized design principle and kinematic modeling of the modularized origami actuators, we design a reconfigurable letter as shown in Fig. 7(d-e), which consists of six bending actuators and rigid linkages joining the actuators. Herein, the origami actuators are actuated individually, and two bending actuators are bonded together to form a two-layer bending actuator, which aims at amplifying the bending angle. As shown in Fig. 7(e), the letter reconfigures from an I-shape to L-shape by actuating one of the two-layer bending actuators. Taking the center of the robot as the origin, the position of the tip, point A in Fig. 7(e), can be computed by

$$ {}^{0}_{A}P = {}^{0}_{1}T\, T_{bend}(\alpha,\gamma)\, T_{bend}(\alpha)\, {}^{3}_{A}P \qquad (5) $$
$$ = \begin{bmatrix} 161.73 \\ 0 \\ 71.73 \\ 1 \end{bmatrix} $$

where ${}^{0}_{1}T$ is computed by substituting parameters in Fig. 7(e) into (1), with h_3 = 50 mm. T_{bend} is derived from (2), with H = 36 mm, γ = 22.5°, and α = 45°. ${}^{3}_{A}P = [0 \quad 0 \quad 140 \quad 1]^T$ is the position of point A in the local coordinate system $x_3y_3z_3$, and ${}^{0}_{A}P$ is the position of point A in the global coordinate system.

Applying negative pressure to all the actuators, the robot will further change its shape from the letter "L" to the letter "C", as shown in Fig. 7(f). Considering the configuration is symmetric, we focus on the lower half to model the kinematics of the system. Then, the position of the tip is computed by

$$ {}^{0}_{A}P = {}^{0}_{1}T\, T_{bend}(\alpha)\, T_{bend}(\alpha)\, {}^{3}_{4}T\, T_{bend}(\alpha)\, {}^{5}_{A}P \qquad (6) $$
$$ = \begin{bmatrix} 122.51 \\ 0 \\ 32.33 \\ 1 \end{bmatrix} $$

Similarly, the transformation matrix ${}^{0}_{1}T$ and T_{bend} are the same as in (5). ${}^{3}_{4}T$ can be computed by substituting parameters in Fig. 7(e) into (1), with h_4 = 60 mm. ${}^{5}_{A}P = [0 \quad 0 \quad 40 \quad 1]^T$ is the position of point A in the local coordinate system $x_5y_5z_5$, with h_5 = 40 mm, and ${}^{0}_{A}P$ is the position of point A in the global coordinate system. This reconfigurable letter verifies the modularized design principle and efficient kinematics model proposed in this paper. It is strongly recommended to use the modularized origami actuators to build locomotive robots in the future.

V. Conclusion

In this study, we proposed a novel concept of modularized origami soft actuators and designed three types of actuators that can generate contraction, bending, and twisting motion, respectively. Akin to the rigid robots, the motion of the proposed origami actuators can be modeled by rigid body kinematics, and complex motions can be achieved by simply assembling the origami actuators rationally and modeled by homogeneous transformations. To prototype the modularized origami actuators with high fidelity, we take the benefits of PVA support material in 3D printing technology to ensure the positioning of PLA panels onto the TPU-coated fabric. Using this prototyping method, these modularized origami actuators can be fabricated in two hours and are able to generate a robust and large range of motion, and also exert high payloads. With prototyped origami actuators, we characterized the payload capability and workspace of the three types of modularized origami actuators. After that, we demonstrated the modularized design principle and efficient kinematics model on a manipulator and a reconfigurable letter.

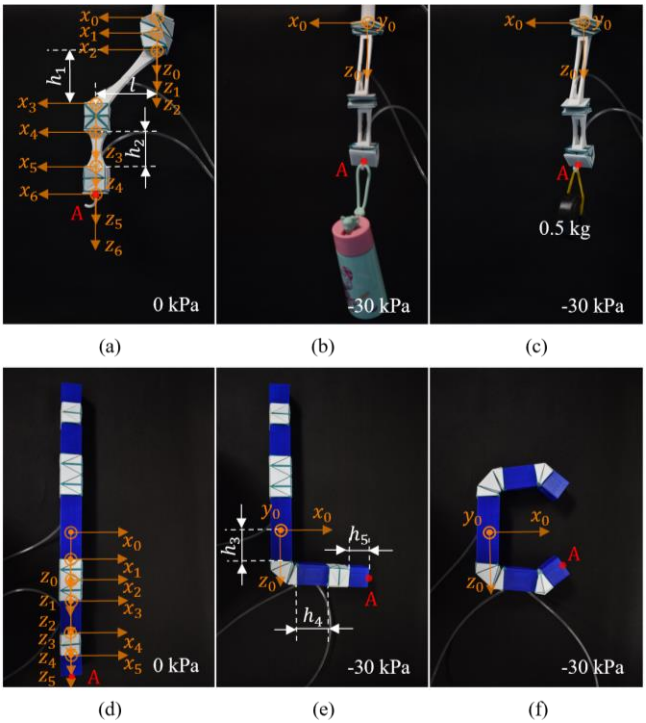

Fig. 7. The demonstration of the modularized design principle and applications on (a-c) a manipulator and (d-f) reconfigurable letter. Herein, (a) and (d) are initial configuration, (b) and (c) are verification for lifting a mug and a 0.5 kg weight, respectively, and (e) and (f) are two activated configurations (letter "L" and letter "C").

The modularized origami actuators are expected to lead the paradigm shifts in the design and modeling of soft robots shortly. However, to bring the proposed modularized origami actuators into real industrial applications, we still need to solve the challenges in materials with high fatigue strength and closed-loop control of the system. In our future study, we will investigate more types of origami actuators and closed-loop control of a soft robot system built by modularized origami actuators.

Acknowledgment

The authors would like to thank Mrs. Hui Wang from the National University of Singapore (Suzhou) Research Institute for her guidance during the experiments.

References

[1] C. Majidi, "Soft robotics: a perspective—current trends and prospects for the future," *Soft robotics,* vol. 1, no. 1, pp. 5-11, 2014.

[2] D. Rus and M. T. Tolley, "Design, fabrication and control of soft robots," *Nature,* vol. 521, no. 7553, pp. 467-475, 2015.

[3] C. Laschi, B. Mazzolai, and M. Cianchetti, "Soft robotics: Technologies and systems pushing the boundaries of robot abilities," *Science robotics,* vol. 1, no. 1, p. eaah3690, 2016.
[4] B. Mosadegh *et al.*, "Pneumatic networks for soft robotics that actuate rapidly," *Advanced functional materials,* vol. 24, no. 15, pp. 2163-2170, 2014.
[5] P. Polygerinos *et al.*, "Modeling of soft fiber-reinforced bending actuators," *IEEE Transactions on Robotics,* vol. 31, no. 3, pp. 778-789, 2015.
[6] E. W. Hawkes, D. L. Christensen, and A. M. Okamura, "Design and implementation of a 300% strain soft artificial muscle," in *2016 IEEE International Conference on Robotics and Automation (ICRA)*, 2016, pp. 4022-4029: IEEE.
[7] J. Wang, Y. Fei, and W. Pang, "Design, modeling, and testing of a soft pneumatic glove with segmented pneunets bending actuators," *IEEE/ASME Transactions on Mechatronics,* vol. 24, no. 3, pp. 990-1001, 2019.
[8] F. Chen and M. Y. Wang, "Design optimization of soft robots: A review of the state of the art," *IEEE Robotics & Automation Magazine,* vol. 27, no. 4, pp. 27-43, 2020.
[9] B. Pawlowski, J. Sun, J. Xu, Y. Liu, and J. Zhao, "Modeling of soft robots actuated by twisted-and-coiled actuators," *IEEE/ASME Transactions on Mechatronics,* vol. 24, no. 1, pp. 5-15, 2018.
[10] A. Shiva *et al.*, "Tendon-based stiffening for a pneumatically actuated soft manipulator," *IEEE Robotics and Automation Letters,* vol. 1, no. 2, pp. 632-637, 2016.
[11] Y. Sun, Y. S. Song, and J. Paik, "Characterization of silicone rubber based soft pneumatic actuators," in *2013 IEEE/RSJ International Conference on Intelligent Robots and Systems*, 2013, pp. 4446-4453: Ieee.
[12] D. Rus and M. T. Tolley, "Design, fabrication and control of origami robots," *Nature Reviews Materials,* vol. 3, no. 6, pp. 101-112, 2018.
[13] N. Turner, B. Goodwine, and M. Sen, "A review of origami applications in mechanical engineering," *Proceedings of the Institution of Mechanical Engineers, Part C: Journal of Mechanical Engineering Science,* vol. 230, no. 14, pp. 2345-2362, 2016.
[14] T. A. Evans, R. J. Lang, S. P. Magleby, and L. L. Howell, "Rigidly foldable origami gadgets and tessellations," *Royal Society open science,* vol. 2, no. 9, p. 150067, 2015.
[15] J. Huang *et al.*, "Modular origami soft robot with the perception of interaction force and body configuration," *Advanced Intelligent Systems,* vol. 4, no. 9, p. 2200081, 2022.
[16] R. V. Martinez, C. R. Fish, X. Chen, and G. M. Whitesides, "Elastomeric origami: programmable paper‐elastomer composites as pneumatic actuators," *Advanced functional materials,* vol. 22, no. 7, pp. 1376-1384, 2012.
[17] J. Santoso, E. H. Skorina, M. Luo, R. Yan, and C. D. Onal, "Design and analysis of an origami continuum manipulation module with torsional strength," in *2017 IEEE/RSJ International Conference on Intelligent Robots and Systems (IROS)*, 2017, pp. 2098-2104: IEEE.
[18] E. Vander Hoff, D. Jeong, and K. Lee, "OrigamiBot-I: A thread-actuated origami robot for manipulation and locomotion," in *2014 IEEE/RSJ International Conference on Intelligent Robots and Systems*, 2014, pp. 1421-1426: IEEE.
[19] S. Wu, Q. Ze, J. Dai, N. Udipi, G. H. Paulino, and R. Zhao, "Stretchable origami robotic arm with omnidirectional bending and twisting," *Proceedings of the National Academy of Sciences,* vol. 118, no. 36, p. e2110023118, 2021.
[20] K. Zhang and K. Althoefer, "Designing origami-adapted deployable modules for soft continuum arms," in *Towards Autonomous Robotic Systems: 20th Annual Conference, TAROS 2019, London, UK, July 3–5, 2019, Proceedings, Part I 20*, 2019, pp. 138-147: Springer.
[21] C. D. Onal, M. T. Tolley, R. J. Wood, and D. Rus, "Origami-inspired printed robots," *IEEE/ASME transactions on mechatronics,* vol. 20, no. 5, pp. 2214-2221, 2014.
[22] H. Zhang, "Mechanics Analysis of Functional Origamis Applicable in Biomedical Robots," *IEEE/ASME Transactions on Mechatronics,* 2021.
[23] C. Jianguo, D. Xiaowei, Z. Ya, F. Jian, and T. Yongming, "Bistable behavior of the cylindrical origami structure with Kresling pattern," *Journal of Mechanical Design,* vol. 137, no. 6, p. 061406, 2015.
[24] C. Jianguo, D. Xiaowei, Z. Yuting, F. Jian, and Z. Ya, "Folding behavior of a foldable prismatic mast with kresling origami pattern," *Journal of Mechanisms and Robotics,* vol. 8, no. 3, p. 031004, 2016.
[25] Y. Chen, H. Feng, J. Ma, R. Peng, and Z. You, "Symmetric waterbomb origami," *Proceedings of the Royal Society A: Mathematical, Physical and Engineering Sciences,* vol. 472, no. 2190, p. 20150846, 2016.
[26] A. E. Forte, D. Melancon, L. M. Kamp, B. Gorissen, and K. Bertoldi, "MuA-Ori: Multimodal actuated origami," *arXiv preprint arXiv:2112.01366,* 2021.
[27] A. Firouzeh and J. Paik, "An under-actuated origami gripper with adjustable stiffness joints for multiple grasp modes," *Smart Materials and Structures,* vol. 26, no. 5, p. 055035, 2017.
[28] C.-P. Chou and B. Hannaford, "Measurement and modeling of McKibben pneumatic artificial muscles," *IEEE Transactions on robotics and automation,* vol. 12, no. 1, pp. 90-102, 1996.